Morphology-Based Multifractal Estimation for Texture Segmentation

Yong Xia, *Student Member, IEEE*, (David) Dagan Feng, *Fellow, IEEE*, and Rongchun Zhao

***Abstract*—Multifractal analysis is becoming more and more popular in image segmentation community, in which the box-counting based multifractal dimension estimations are most commonly used. However, in spite of its computational efficiency, the regular partition scheme used by various box-counting methods intrinsically produces less accurate results. In this paper, a novel multifractal estimation algorithm based on mathematical morphology is proposed and a set of new multifractal descriptors, namely the local morphological multifractal exponents is defined to characterize the local scaling properties of textures. A series of cubic structure elements and an iterative dilation scheme are utilized so that the computational complexity of the morphological operations can be tremendously reduced. Both the proposed algorithm and the box-counting based methods have been applied to the segmentation of texture mosaics and real images. The comparison results demonstrate that the morphological multifractal estimation can differentiate texture images more effectively and provide more robust segmentations.**

***Index Terms*—Fractal dimension, image segmentation, mathematical morphology, multifractal estimation.**

I. Introduction

FRACTAL geometry, as initially developed and explored by Mandelbrot [1], [2], does not assume that the studied objects have good properties of continuity and smoothness, and thus enables the characterization of irregularity and complexity that may not be treated in general by Euclidean geometry. Since Pentland [3] presented evidence that most natural surfaces are spatially isotropic fractals and the intensity images of these surfaces are also fractals, fractal analysis has been successfully applied to many fields of digital image processing [4]–[6]. It offers the potential of unifying and simplifying various two dimensional texture descriptions, as well as the possibility of interpreting them in terms of three dimensional structure of the image.

Manuscript received October 14, 2003; revised March 8, 2005. This work was supported by an HK-RGC grant, an ARC grant, and by the NSFC under Grant 60141002. The associate editor coordinating the review of this manuscript and approving it for publication was Dr. Eli Saber.

Y. Xia is with the Center for Multimedia Signal Processing, Department of Electronic and Information Engineering, Hong Kong Polytechnic University, Hong Kong, with the School of Information Technologies, University of Sydney, Sydney NSW2006, Australia, and also with the School of Computer, Northwestern Polytechnical University, Xi'an 710072, China (e-mail: yxia@it.usyd.edu.au).

D. Feng is with the School of Information Technologies, University of Sydney, Sydney NSW2006, Australia, and also with the Center for Multimedia Signal Processing, Department of Electronic and Information Engineering, Hong Kong Polytechnic University, Hong Kong (e-mail: feng@it.usyd.edu.au).

R. Zhao is with the School of Computers, Northwestern Polytechnical University, Xi'an 710072, China (e-mail: rczhao@nwpu.edu.cn).

Digital Object Identifier 10.1109/TIP.2005.863029

Due to its relative insensitivity to scaling transformation and strong correlation with the judgment of surface roughness by human vision system (HVS) [3], the fractal dimension has been widely used in texture segmentation [7]–[16]. However, a number of researchers have argued that a single fractal dimension may not fully represent and discriminate textures. Some studies [17] on different textures showed that, despite of obvious visual differences, the estimated fractal dimensions remained quite identical. The reason lies in the fact that the fractal dimension can only characterize self-similarity in ideal cases. Nevertheless, most real textures are merely semi-fractals and have anisotropic and inhomogeneous scaling properties [7], which can hardly be successfully characterized by the fractal dimension. Therefore, a set of measures, instead of only one, should be used to describe statistically the same phenomenon in different scales in order to achieve efficient texture analysis. This generalization leads to the idea of multifractal analysis (MFA).

As a natural extension of the fractal modeling, multifractal analysis has drawn much more attention in the image processing society in recent years [18]–[27]. Many multifractal features have been developed, among which multifractal dimensions are the most popular ones. Known as a continuous spectrum of exponents, multifractal dimensions provide a simple yet powerful way to probe statistically the inhomogeneous scaling properties of fractal set, and has been shown to be distinct with respect to the texture contents of images.

There are several methods available to estimate the multifractal dimensions of images. One of the commonly used methods proposed by Chaudhuri and Sarkar [10] is based on the differential box-counting (DBC) algorithm [9]. Instead of directly measuring an image surface, the measures at different scales are obtained by means of counting the minimum number of boxes of different size, which can entirely cover the whole surface. Taking account that obtaining the optimal box number N_ε usually involves complex optimization, this method adopts the regular partition scheme to gain an approximation of N_ε. The process can be detailed as follows. For a given scale ε, an $M \times M$ image is partitioned into grids of size $\varepsilon \times \varepsilon$. On each grid, there is a column of $\varepsilon \times \varepsilon \times \varepsilon'$ boxes, where $\varepsilon' = \lfloor \varepsilon \times G/M \rfloor$ and G is the maximum gray level. The image is viewed as a three-dimensional (3-D) surface, where (i, j) denotes the 2-D position and the third coordinate z denotes the gray level of the corresponding pixel. Given the maximum and minimum gray levels in the $(i, j)^{\text{th}}$ grid fall in the v^{th} and u^{th} boxes respectively, the number of boxes needed to cover the image surface on that grid is calculated as

$$n_\varepsilon(i, j) = v - u + 1 \tag{1}$$

and the total number of boxes needed to cover the whole surface can then be approximately estimated as follows:

$$\widetilde{N}_\varepsilon = \sum_{i,j} n_\varepsilon(i,j). \tag{2}$$

In order to describe the distribution of different subfractals, a measure $\mu_\varepsilon(i,j)$ is defined on the grid as

$$\mu_\varepsilon(i,j) = \frac{n_\varepsilon(i,j)}{\widetilde{N}_\varepsilon}. \tag{3}$$

The partition and estimation are performed for different scales, and the multifractal dimension of order q can be estimated by

$$D_q \equiv \frac{1}{1-q} \lim_{\varepsilon \to 0} \frac{\ln\left[\sum_{i,j} \mu_\varepsilon(i,j)^q\right]}{\ln\left(\frac{1}{r}\right)} \tag{4}$$

where $r = \varepsilon/M$.

It is obvious that the box number $\widetilde{N}_\varepsilon$ counted by this scheme is only a rough approximation of the optimal one. Feng *et al.* [28] demonstrated that this method caused under-counting at a smaller scale and over-counting at a larger scale and thus produced a decreased estimation of fractal features. Therefore, though quite effective, the box-counting based algorithm may lead to less precise multifractal estimations. More recently, Du and Yeo [27] have proposed a novel modification to this approach, which combines the idea of the relative differential box-counting (RDBC) algorithm [11] and the multifractal estimation based on the gliding-box method [29]. Although resulting in better accuracy, the modified approach can hardly fully eliminate the intrinsical estimation error caused by the box-counting scheme.

Abandoning the means of box-counting, this paper adopts the basic morphological operations to directly measure an image surface and hence proposes a novel multifractal estimation algorithm to characterize texture images. The quality of the estimation is evaluated on both synthetic images and various natural textures from the Brodatz album [30]. Comparative experiments have been carried out by applying our multifractal texture descriptors and other two box-counting based multifractal dimensions to differentiate the mosaics of Brodatz textures and the images of natural scenes.

II. Morphology-Based Multifractal Estimation

Fractal estimation is, as described by Mandelbrot, based on the idea of "measure the fractal set at different scales." The fractal dimension can be obtained from the relation between the measures acquired and the scales used. He gives, as an example, the calculation of the length of the British coastline [2]. Let the center of a small disk with radius ε follow the coastline to form a strip of width 2ε, within which all the points have the same property: its distance to the coastline is less than the radius ε. The suggested length $L(\varepsilon)$ of the coastline can be expressed by the area of the strip divided by 2ε. As ε decreases, $L(\varepsilon)$ increases. For a fractal curve, he concludes that the following equation holds well:

$$L(\varepsilon) = C\varepsilon^{1-s} \tag{5}$$

where C is a constant and s is the desired fractal dimension of the curve.

When Mandelbrot's original idea is extended to surface area estimation, it is natural to suppose that all points with distance to the surface of no more than ε form a 3-D object. The area $A(\varepsilon)$ of the surface is the volume of the object divided by 2ε, and the fractal dimension of the surface can be estimated from power law followed by $A(\varepsilon)$ and ε. In order to form the 3-D object and measure its volume, Peleg *et al.* [7] iteratively constructed blankets, Sarkar and Chaudhuri [9] piled the image surface with boxes of different scales. However, it can be achieved in a more straightforward and accurate way by adopting the operations of the mathematical morphology.

Since it was developed by Matheron and Serra [31], Mathematical morphology has been a useful tool for image analysis. Through eliminating the details whose scale is less than that of the structure element (SE), it provides us the ability to observe and measure an image at different scales. Samarabandu *et al.* [32] have proposed a morphological method to estimate the fractal dimension of an image, which has superior performance as compared to popular fractal dimension estimations. However, in order to reduce the time cost, this method use only one invariable SE to measure the image surface by iteratively dilating it, which limits the improvement of the estimation accuracy.

In our multifractal estimation method, a series of SEs of different scales is used to measure the image surface. Similarly, an $M \times N$ image is considered to be a 3-D surface X, which can be defined as a set of triplets $\{\langle i,j,f(i,j)\rangle; i = 1,2,\cdots,M; j = 1,2,\cdots,N\}$. For every scale ε, the SE Y_ε is also given as a set of triplets $\{\langle i_{\varepsilon k}, j_{\varepsilon k}, z_{\varepsilon k}\rangle; k = 1,2,\cdots,P_\varepsilon\}$, where P_ε is the number of elements in Y_ε. The dilation of X with Y_ε at pixel (i,j) is calculated as

$$f_\varepsilon(i,j) = \max_{k=1,2,\cdots,P_\varepsilon} \{f(i+i_{\varepsilon k}, j+j_{\varepsilon k}) + z_{\varepsilon k}\}. \tag{6}$$

The dilation $X \oplus Y_\varepsilon$ will result in a 3-D surface, which contains all the points with a distance ε to the upper side of the original surface X. In 3-D space, if we define the distance between points (i,j,k) and (i',j',k') as

$$d(i,j,k,i',j',k') = \sqrt{(i-i')^2 + (j-j')^2 + (k-k')^2}. \tag{7}$$

Consequently, the SE used in the dilation will be a sphere, whereas a different distance definition may lead to a different SE. In our approach, the distance is defined as

$$d(i,j,k,i',j',k') = \max\left\{|i-i'|, |j-j'|, \frac{1}{\beta}|k-k'|\right\} \tag{8}$$

whereupon a cubic SE will be obtained, and that means

$$z_{\varepsilon k} \equiv \beta\varepsilon, \quad k = 1,2,\cdots,P_\varepsilon. \tag{9}$$

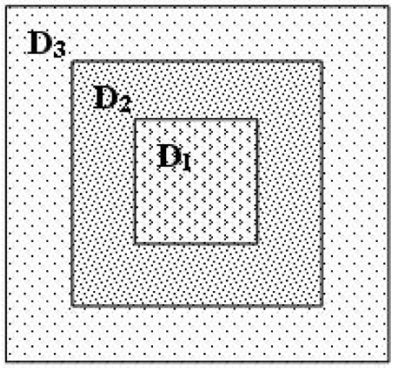

Fig. 1. Extended support of SEs at different scales.

The coefficient β determines the shape of the SE and thereby called the shape factor. Substituting the new value of $Z_{\varepsilon k}$ into (6), we find

$$f_\varepsilon(i,j) = \max_{k=1,2,\cdots,P_\varepsilon} \{f(i+i_{\varepsilon k}, j+j_{\varepsilon k}) + \beta\varepsilon\}. \quad (10)$$

It is obvious that, taking advantage of the cubic SE, the second term on the right hand of (10) is independent of the indicator k. Let $f'_\varepsilon(i,j) = \max_{k=1,2,\cdots,P_\varepsilon} f(i+i_{\varepsilon k}, j+j_{\varepsilon k})$, and (10) can be rewritten

$$f_\varepsilon(i,j) = f'_\varepsilon(i,j) + \beta\varepsilon. \quad (11)$$

For different scales, $f'_\varepsilon(i,j)$ can be calculated iteratively

$$f'_{\varepsilon+1}(i,j) = \max\left\{f'_\varepsilon(i,j), \max_{(i',j')\in D_{\varepsilon+1}} f(i',j')\right\} \quad (12)$$

where D_ε represents the extended support of the SE at scale ε, as shown in Fig. 1. Initially, $f'_0(i,j) = 0$ for all i,j. By this means, the computation cost of $f'_\varepsilon(i,j)$ for all scales equals to that for the maximum scale.

Similar to the definition of the multifractal measure used in the DBC-based method [10] and the RDBC-based method [27], a local natural measure $\mu_\varepsilon(i,j)$ is defined in a window of size $W \times W$ as

$$\mu_\varepsilon(i,j) = \frac{|f_\varepsilon(i,j) - f(i,j)|}{\sum_{i,j}^{W} |f_\varepsilon(i,j) - f(i,j)|}. \quad (13)$$

Then the measure of order q at scale ε can be calculated as

$$I(q,\varepsilon) \equiv \alpha \sum_{i,j}^{W} \mu_\varepsilon(i,j)^q \quad (14)$$

where

$$\alpha = \frac{\sum_{i,j}^{W} |f_\varepsilon(i,j) - f(i,j)|}{\varepsilon}. \quad (15)$$

As a multifractal measure, $I(q,\varepsilon)$ must satisfy the following power law:

$$I(q,\varepsilon) \sim \varepsilon^{\tau(q)}, \quad -\infty < q < \infty. \quad (16)$$

Subsequently, a set of multifractal texture descriptors, namely the local morphological multifractal exponents (LMME), are defined as follows:

$$L_q = \frac{1}{|q|} \lim_{\varepsilon\to 0} \frac{\ln(I(q,\varepsilon))}{\ln\left(\frac{1}{\varepsilon}\right)}, \quad q \neq 0. \quad (17)$$

Plot $\ln(I(q,\varepsilon))$ versus $\ln(1/\varepsilon)$ for a given set of scales and the limitation in (17) can be estimated by the gradient of the line that fits the plot. The coefficient α is added to assure that the morphological fractal dimension is given by L_1. In the following experiments, the window size w is set to be 11, the shape factor β is 3, and the scales ε of SE are 2, 3, 4, 5, and 6, respectively.

III. Estimation Evaluation

In this section, we use two sets of images to test the performance of our proposed multifractal estimation algorithm. Image Set I consists of ten synthetic textured images of size 256 × 256, which are 2-D discrete Gaussian grids each with a mean of 128 and standard deviation of 1, 4, 8, 16, 24, 32, 48, 60, 84, and 128 [9], [11]. Those samples are denoted by $\mathrm{S1}, \mathrm{S2}, \ldots, \mathrm{S10}$ and half of them are shown in Fig. 2. The generated gray-levels are truncated so that they lie in the range [0, 255] and the exact standard deviations of those images are 1.04, 4.01, 7.98, 16.05, 23.89, 32.11, 47.58, 57.93, 74.61, and 91.51, respectively. Image Set II consists of 12 natural textures of size 256 × 256, which are randomly chosen from Brodatz album [30]. Those samples are denoted by $\mathrm{T1}, \mathrm{T2}, \mathrm{T}\ldots, \mathrm{T12}$ and are shown in Fig. 3.

Similar to the experiments in [10] and [11], we use the distance error to evaluate the quality of the proposed estimation. Plotting $\ln(I(q,\varepsilon))$ versus $\ln(1/\varepsilon)$ for several different scales and typically those points will lie on a straight line. Let $\mathbf{y} = m\mathbf{x} + c$ is the fitted line, $\mathbf{y}$ denotes $\ln(I(q,\varepsilon))$ and $\mathbf{x}$ denotes $\ln(1/\varepsilon)$. The quality of the estimation may be evaluated by the fitted error, which can be expressed as the root mean-square distance of the points from the fitted line

$$DE = \frac{\sqrt{\sum_{i=1}^{n} \frac{(mx_i + c - y_i)^2}{(1+m)^2}}}{n} \quad (18)$$

where n is the number of scales used.

For every image, the proposed estimation is performed at each pixel (i,j) using a moving window of size 11 × 11 centered on (i,j). The results are averaged over all pixels to decrease the impact of randomness. Some components of the average LMME spectrum, respectively $L_{-3}, L_{-2}, L_{-1}, L_1, L_2$, and L_3, together with the average fitted errors, are shown in Figs. 4 and 5.

As for the synthetic textures, the bigger the standard deviation, the more rugged the image surface is, and the larger fractal feature will usually be expected. It is revealed from Fig. 4(a) that our LMME spectrum can successfully capture this trend. However, the performance of each component with respect to different order q is of significant difference. Comparing with L_2 and L_3, the estimations of L_{-3}, L_{-2}, L_{-1} and L_1 occupy a

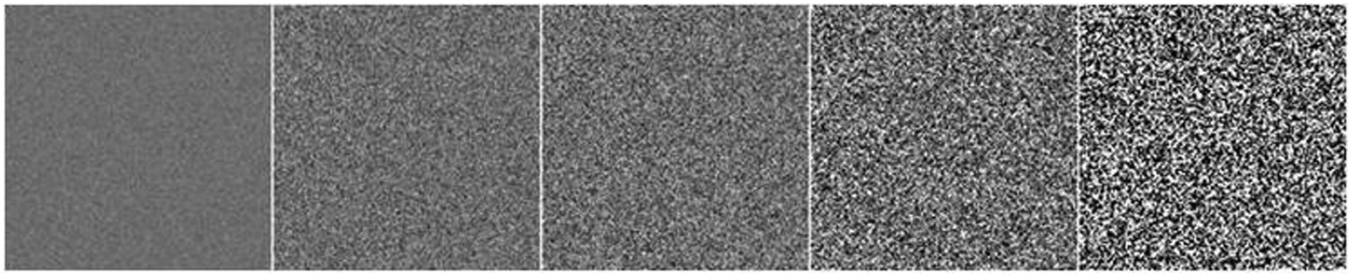

Fig. 2. Five samples of the synthetic images: name and the standard deviations.

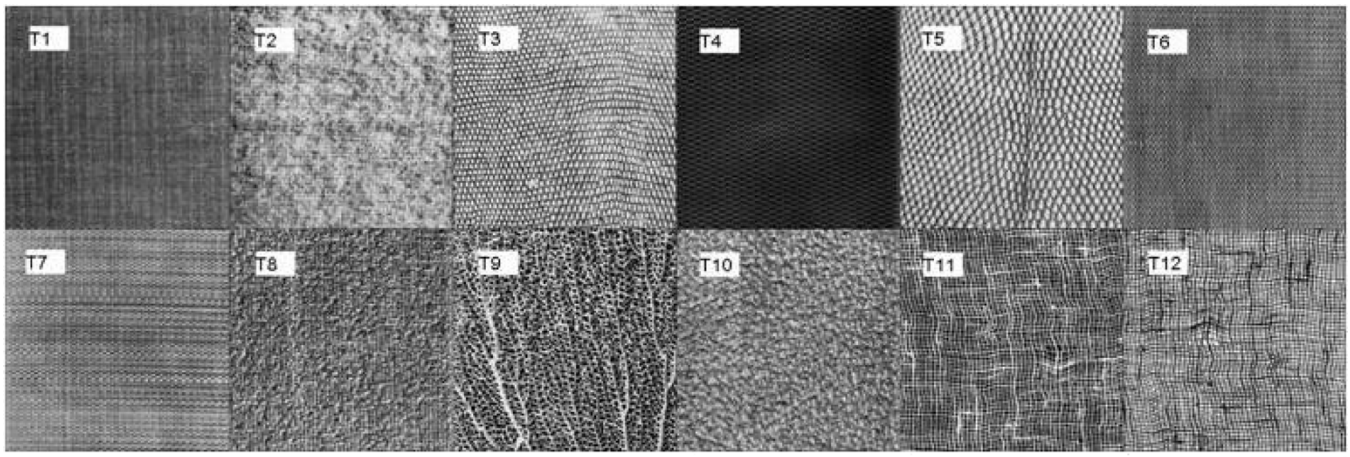

Fig. 3. Twelve natural textures from Brodatz album. Their name and corresponding positions are shown in the table below the figure.

wider dynamic range, which demonstrates a better ability to distinguish textures. The same conclusion can also be drawn from Fig. 5(a).

As depicted in the previous section, the multifractal measures $I(q, \varepsilon)$ used in the deduction of the local morphological multifractal exponents is defined by analogy with the DBC-based algorithm. Given that $I(q, \varepsilon)$ effectively characterizes the multifractal properties of an image surface, it must follow the power law with scale ε. Consequently, $\ln(I(q, \varepsilon))$ and $\ln(1/\varepsilon)$ will exhibit a perfect linear relationship, which must result in an ideal linear fit and a low fitted error. As illustrated in Figs. 4(b) and 5(b), the average distance errors of the proposed estimation are as low as that of popular estimations of fractal dimension, which are, as reported in [10] and [11], ranging from 0.001 to 0.074. The satisfying results demonstrate that the proposed morphological measures can certainly follow the desired power law and the proposed estimation is able to successfully characterize the local scaling properties of texture images.

IV. Experimental Results

To assess the ability of the proposed multifractal estimation to differentiate various natural textures, the obtained LMME spectrum has been applied to the segmentation of texture images. To decrease the complexity of the classifier, only three components of the LMME spectrum $\{L_{-2}, L_{-1}, L_1\}$, which exhibit wider dynamic ranges in Figs. 4 and 5, are used as the features in our experiments. For every pixel, the multifractal features are computed in a slipping window of size 11×11 centered on that point. The segmentation is essentially based on the fuzzy C-means (FCM) algorithm [33], which is able to classify the pixels into a specified number of regions by clustering those features.

Besides our LMME estimation, other two groups of multifractal dimensions are also used as image features in our comparative experiments. One is estimated by the method based on differential box-counting and therefore denoted as MDBC, the other is presented by generalizing the relative differential box-counting algorithm and denoted as MRDBC. The MDBC features are initially developed by Chaudhuri and Sarkar [10], and three components of them ($q = -5, 1, 5$) have been used by Li *et al.* [26] to segment mosaic textures. The MRDBC features are first introduced by Du and Yeo [27], and four components of them ($q = -1, 0, 1, 2$) have been applied to the segmentation of remote sensing images. Both of those two group of features are calculated within a window of size 17×17. In following experiments, every test image is segmented by three different approaches, and the results are compared through the error percentage of the incorrectly classified pixels. Since these experiments are aimed to evaluate the ability of different multifractal descriptors to differentiate various textures, those three segmentation methods share the same scheme and the same FCM-based

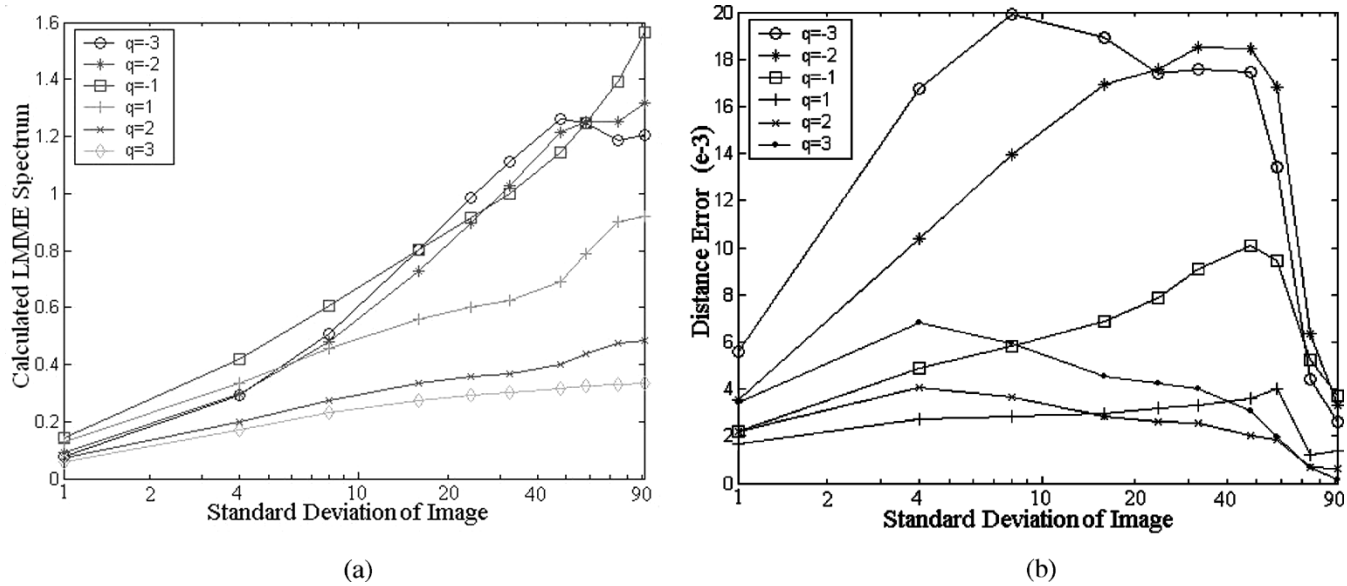

Fig. 4. Morphology-based multifractal estimation on synthetic textures. (a) LMME spectrum and (b) distance error.

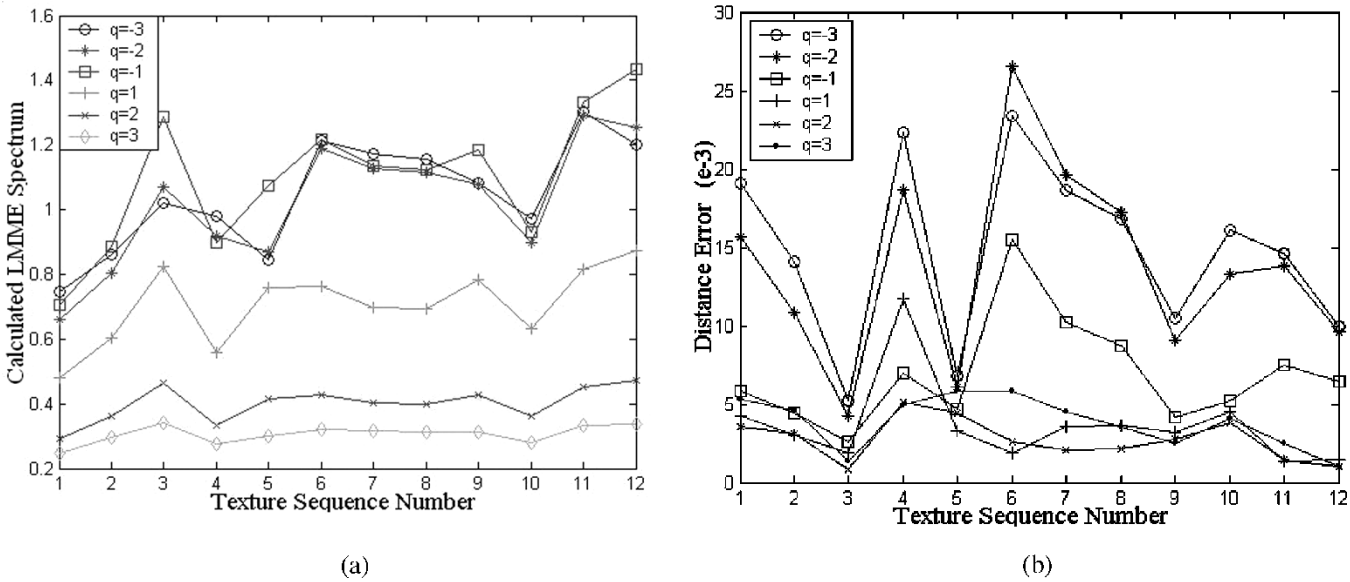

Fig. 5. Morphology-based multifractal estimation on Brodatz textures. (a) LMME spectrum and (b) distance error.

algorithm. The only distinctions of them are the image features. For this reason, they are referred by the notation of the corresponding features. It should be noted that other unsupervised classifier, such as the self-organization map (SOM) [34], may bring better segmentation result, but it will not influence our evaluation of those multifractal texture descriptors. Discussing the impact of different classifiers is obviously beyond the scope of this paper.

The first comparative experiment has been performed on the image database named as MII, which is generated by using the 12 Brodatz textures shown in Fig. 3. Each texture is combined with every other texture, thus we totally have 66 test images, each of which is a mosaic of two textures with a size of 256×256 and a dynamic range of 256 gray levels. Three example test cases (MII1 to MII3) are shown in the left column of Fig. 6. The right column illustrates the results of the proposed LMME method and the two middle columns show the results obtained by applying the MDBC method and the MRDBC method. Table I gives the segmentation errors of the results shown in Fig. 6. The average error over the whole database is presented in Table II. Generally, the proposed LMME spectrum is preferable to other multifractal dimensions, which are fail to locate accurate boundaries separating the regions.

To demonstrate the advantage of the proposed texture descriptor in differentiating textures of more than two classes, the second comparative experiment has been carried out. This experiment is similar to the previous one, except that it uses the test image set MIV, which consists of 495 mosaics of four different textures with a size of 512×512. Those test images are generated by combining each four patterns chosen from the 12 textures shown in Fig. 3. Four example test cases, together with their corresponding segmentation results, are pre-

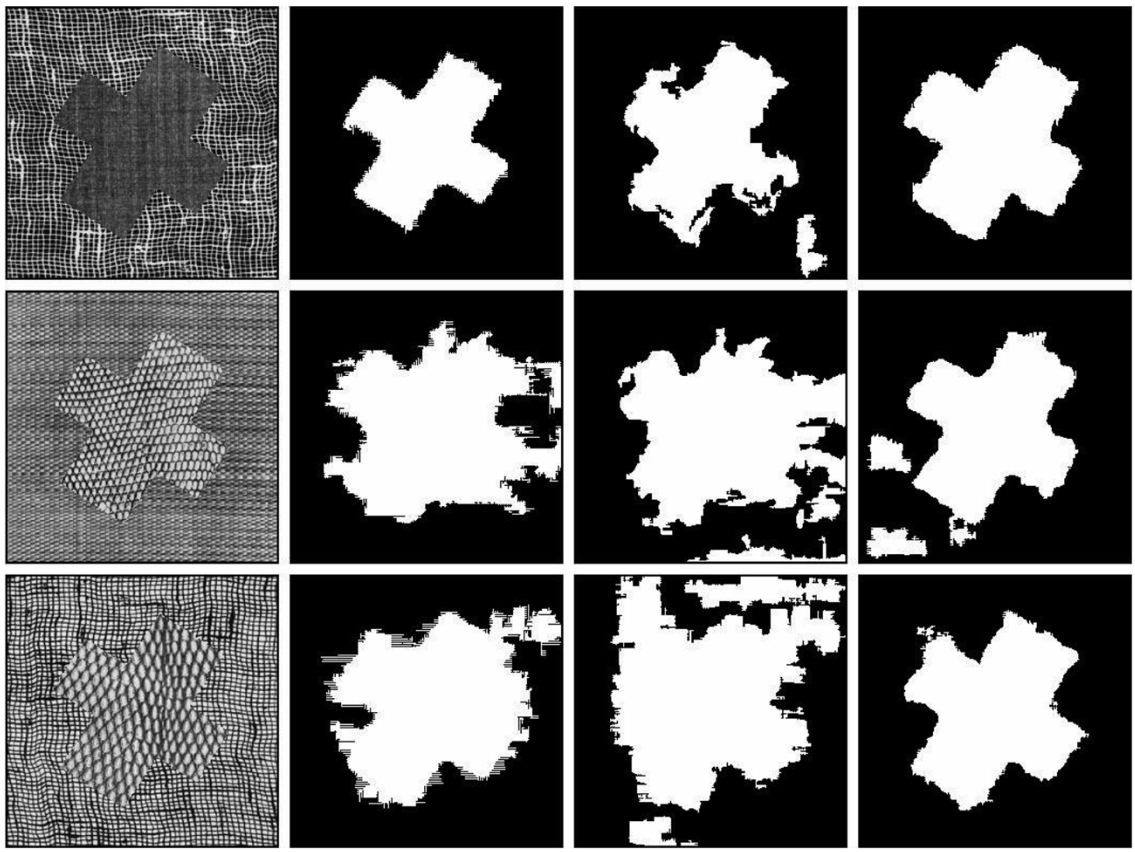

Fig. 6. Three test cases of mosaics of two textures (MII1–MII3) and their segmentation by applying (the second column) the MDBC method, (the third column) the MRDBC method and (right column) the proposed LMME method.

TABLE I
ERROR PERCENTAGE OF INCORRECTLY CLASSIFIED PIXELS (MII1-MII3)

Image Index	Texture Components	Segmentation Methods		
		MDBC	MRDBC	LMME
M1	D16 vs. D103	4.2%	6.5%	3.0%
M2	D22 vs. D55	13.4%	17.0%	5.3%
M3	D35 vs. D104	11.5%	22.9%	3.1%

TABLE II
AVERAGE ERROR PERCENTAGE OF INCORRECTLY CLASSIFIED PIXELS FOR DATABASE MII

Methods	MDBC	MRDBC	LMME
Average Errors	18.61%	20.42%	14.58%

sented in Fig. 7. All segmentation results are shown using arbitrarily selected gray level to highlight different regions. Fig. 8 compares the error percentage of the incorrectly classified pixels obtained by applying different segmentation methods to each of twenty randomly chosen example test images. The averaged errors over the entire database are listed in Table III. Although not superior to the MRDBC features in some cases, the proposed LMME spectrum shows the best discrimination ability and corresponding segmentation method achieves the least overall segmentation error. This is completely in accordance to the results reported in the previous experiment.

Next, we apply the presented comparative experiment to a number of real images. The segmentation of textures in these images is subjective. In Fig. 9, we show the segmentation by the MDBC method, the MRDBC method, and the proposed method for a picture of road, a grassland scene, a crowded stadium, and a face image of a chimpanzee. The results presented from the segmentation scheme, which uses the proposed LMME spectrum are shown in the right column. In all cases, the segmented regions seem to, on the whole, agree with the regions we would perceived as distinct if we try not to make use of semantics like "sky," "grass," "trees," "crowd," etc. Unfortunately, in case of other multifractal features are used, the results are a bit worse, as shown in the two middle columns of Fig. 9.

Generally, multifractal-based image segmentation algorithms are very time consuming. In our approach, we abandoned the complicated box-counting process and adopted the mathematical morphological operators instead to measure the image surface. Through delicately selecting the SE and iteratively dilating the image, the proposed method successfully reduced the computational burden. Table IV gives the average computational time required by the above three segmentation methods in the first two experiments (Intel Pentium III, 871 MHz processor). As shown in the right three columns of the table, the entire time of segmentation depends on many factors, such as image size and how many features are used. To fairly compare the computational expense of those multifractal estimation methods, we also present the average time needed for calculating every single feature, which is the total time of feature extraction divided by

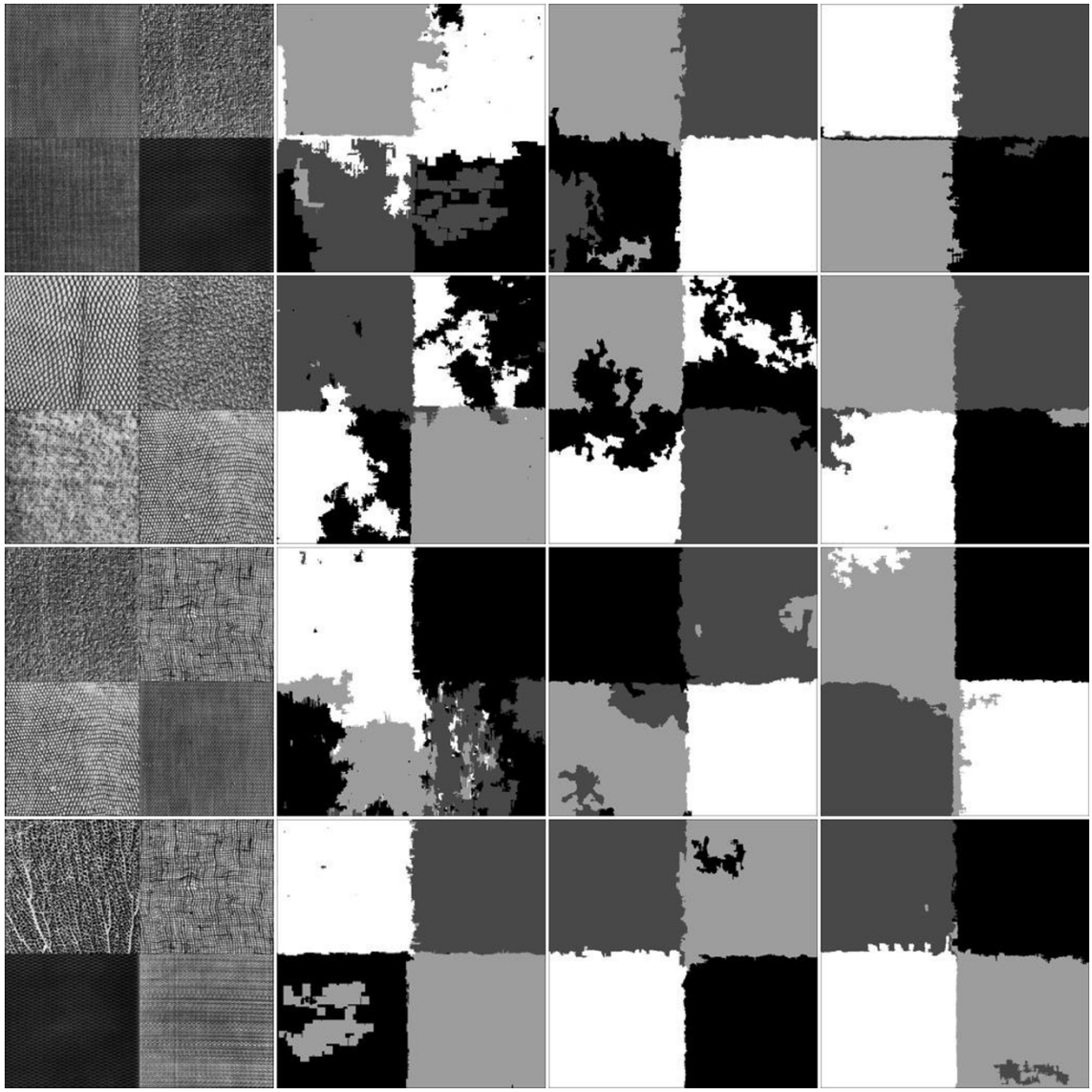

Fig. 7. Four test cases of mosaics of four textures (MIV1–MIV4) and their segmentation by applying (the second column) the MDBC method, (the third column) the MRDBC method and (right column) the proposed LMME method.

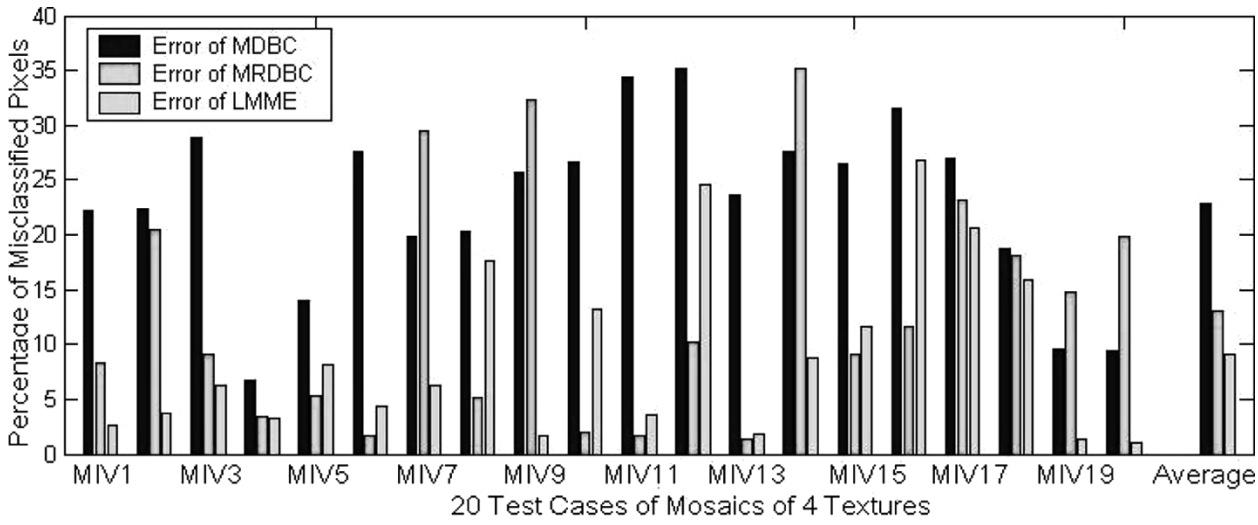

Fig. 8. Error percentage of incorrectly classified pixels (MIV1-MIV20).

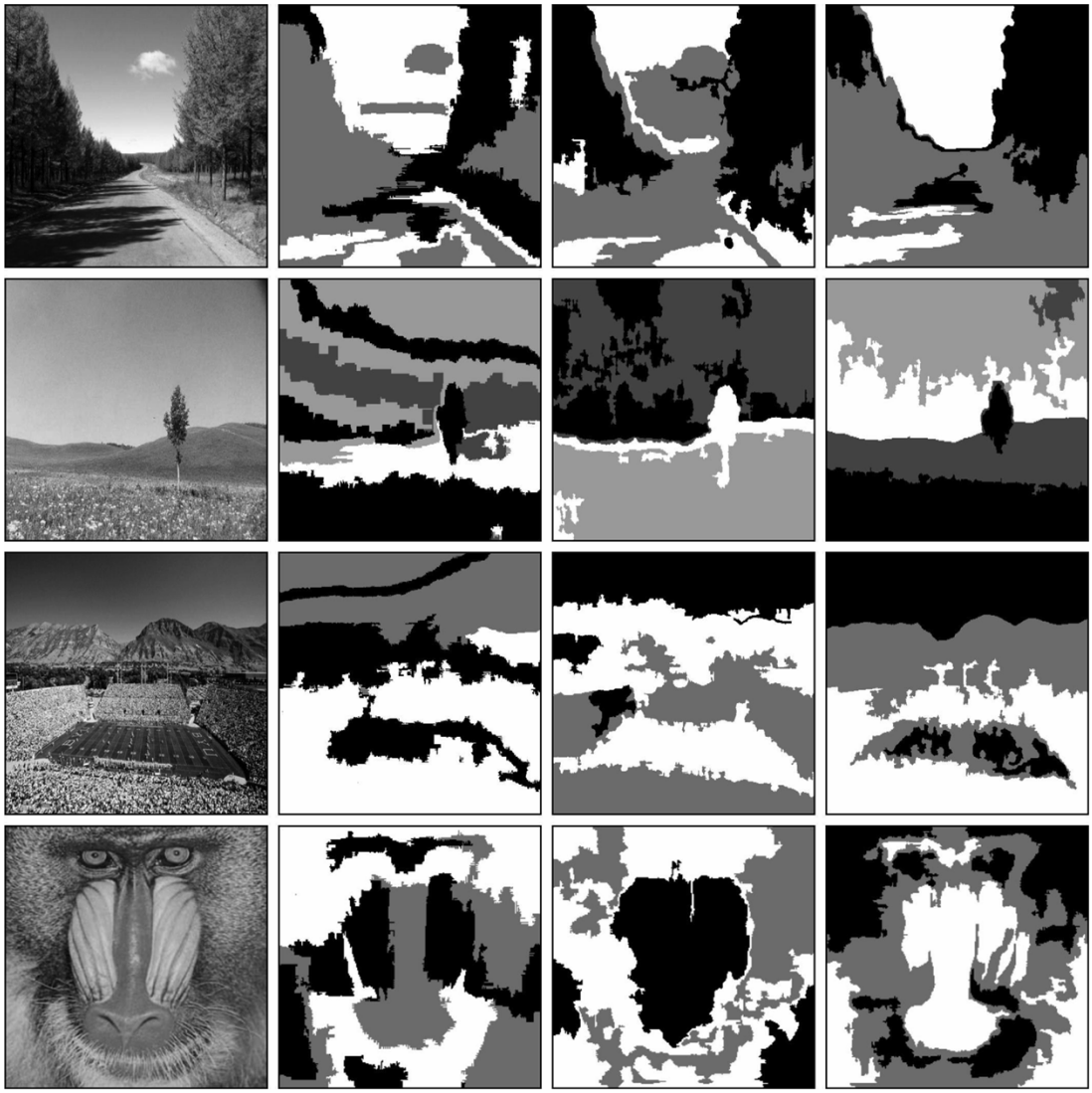

Fig. 9. Four real images and their segmentation by using (the second column) MDBC features, (the third column) MRDBC features and (right column) the proposed LMME spectrum.

TABLE III
AVERAGE ERROR PERCENTAGE OF INCORRECTLY CLASSIFIED PIXELS FOR DATABASE MIV

Methods	MDBC	MRDBC	LMME
Average Errors	22.37%	12.38%	10.63%

the image size and the feature dimension. From Table IV, we can conclude that the computational cost decreased substantially when the proposed LMME features are used.

V. CONCLUSION

Theoretically, multifractal features can successfully describe many structural properties of texture, e.g., coarseness, regularity, etc., which are important parameters in the human visual experience. Most work in the past on multifractal analysis has been concerned with the box-counting scheme. Nevertheless, the mathematical morphology may bring us a more straightforward and accurate way to achieve this goal.

In this paper, a morphology-based multifractal estimation algorithm has been proposed, and as a result, a set of new multifractal texture descriptors has been presented. By means of mathematical morphology, the novel algorithm delicately avoids the drawback of various box-counting methods and thus achieves better accuracy in characterizing the local scaling properties of a texture image. The cubic SE and the iterative dilation scheme used in our approach substantially reduce the computational expense of morphological operations. We evaluated the quality of the proposed multifractal estimation for both the synthetic texture and the natural texture. It reveals that the estimation error is considerably small. The performance of the presented texture descriptors is compared with that of two popular multifractal dimensions on texture mosaics and real images. The experimental results illustrate that the features derived from the proposed multifractal analysis approach has a better ability to differentiate various textures.

TABLE IV
COMPUTATION TIME OF THE THREE SEGMENTATION METHODS ON THE DATABASE MII AND MIV

Image Database	Average Time Per Feature			Average Time of Segmentation		
	MDBC	MRDBC	LMME	MDBC	MRDBC	LMME
M (256×256)	78.36 μs	514.29 μs	39.29 μs	16.654s	137.107s	8.803s
M (512×512)	77.97 μs	497.70 μs	39.18 μs	64.454s	525.813s	34.650s

ACKNOWLEDGMENT

The authors would like to thank Prof. M. Petrou, University of Surrey, and Prof. Z. Yanning, Northwestern Polytechnical University, for their helpful comments. The authors would also like to thank the reviewers for their valuable comments which have improved the presentation of this paper.

REFERENCES

[1] B. B. Mandelbrot, "How long is the coast of Britain? Statistical self-similarity and fractal dimension," *Science*, vol. 156, pp. 636–638, 1967.
[2] ——, *The Fractal Geometry of Nature*. New York: Freeman, 1983.
[3] A. P. Pentland, "Fractal based description of natural scenes," *IEEE Trans. Pattern. Anal. Mach. Intell.*, vol. PAMI-6, no. 6, pp. 661–674, Jun. 1984.
[4] M. Ghazel, G. H. Freeman, and E. R. Vrscay, "Fractal image denoising," *IEEE Trans. Image Process.*, vol. 12, no. 12, pp. 1560–1578, Dec. 2003.
[5] B. Wohlberg and G. De Jager, "A review of the fractal image coding literature," *IEEE Trans. Image Process.*, vol. 8, no. 12, pp. 1716–1729, Dec. 1999.
[6] T. J. Dennis and N. G. Dessipris, "Fractal modeling in image texture analysis," *Proc. Inst. Elect. Eng. Radar Signal Process.*, vol. 136, no. 5, pp. 227–235, Oct. 1989.
[7] S. Peleg, J. Naor, R. Hartley, and D. Avnir, "Multiple resolution texture analysis and classification," *IEEE Trans. Pattern Anal. Mach. Intell.*, vol. PAMI-6, no. 6, pp. 518–523, Jun. 1984.
[8] N. Sarkar and B. B. Chaudhuri, "Multifractal and generalized dimensions of gray-tone digital images," *Signal Process.*, vol. 42, pp. 181–190, Mar. 1995.
[9] ——, "An efficient differential box-counting approach to compute fractal dimension of image," *IEEE Trans Syst. Man Cybern.*, vol. 24, no. 1, pp. 115–120, Jan. 1994.
[10] B. B. Chaudhuri and N. Sarkar, "Texture segmentation using fractal dimension," *IEEE Trans. Pattern Anal. Mach. Intell.*, vol. 17, no. 1, pp. 72–77, Jan. 1995.
[11] X. C. Jin, S. H. Ong, and S. H. Jayasooriah, "A practical method for estimation fractal dimension," *Pattern Recognit. Lett.*, vol. 16, pp. 457–464, May 1995.
[12] Y. Liu and Y. Li, "Image feature extraction and segmentation using fractal dimension," in *Proc. ICSP*, Seoul, Korea, Aug. 26–28, 1997, pp. 975–979.
[13] T. A. Runkler and J. C. Bezdek, "Image segmentation using fuzzy clustering with fractal features," in *Proc. IEEE Int. Conf. Fuzzy Systems*, Barcelona, Spain, Jul. 1–5, 1997, pp. 1393–1398.
[14] J. You, S. Hungnahally, and A. Sattar, "Fractional discrimination for texture image segmentation," in *Proc. IEEE Int. Conf. Image Processing*, Beijing, China, Oct. 28–31, 1997, pp. 220–223.
[15] R. Fazel-Rezai and W. Kinsner, "Texture analysis and segmentation of images using fractals," in *Proc. IEEE Canadian Conf. Electrical Computer Engineering*, May 9–12, 1999, pp. 786–791.
[16] S. Novianto, L. Guimaraes, Y, Suzuki, J. Maeda, and V. V. Anh, "Multiwindowed approach to the optimum estimation of the local fractal dimension for natural image segmentation," in *Proc. IEEE Int. Conf. Image Processing*, Kobe, Japan, Oct. 24–28, 1999, pp. 222–226.
[17] R. Voss, "Random fractals: Characterization and measurement," in *Scaling Phenomena in Disordered Systems*, R. Pynn and A. Skjeltorp, Eds. New York: Plenum, 1986.
[18] F. Arduini, S. Fioravanti, and D. D. Giusto, "A multifractal-based approach to natural scene analysis," in *Proc. IEEE Int. Conf. Acoust., Speech, Signal Processing*, Apr. 14–17, 1991, pp. 2681–2684.
[19] J. L. Vehel, P. Mignot, and J. P. Berroir, "Multifractals, texture, and image analysis," in *Proc. CVPR*, Jun. 15–18, 1992, pp. 661–664.
[20] K. Uma, K. R. Ramakrishnan, and G. Ananthakrishna, "Image analysis using multifractals," in *Proc. IEEE Int. Conf. Acoust., Speech, Signal Processing*, May 7–10, 1996, pp. 2188–2190.
[21] P. Martinez, D. Schertzer, and K. K. Pham, "Texture modelization by multifractal processes for SAR image segmentation," in *Proc. Radar*, Oct. 14–16, 1997, pp. 135–139.
[22] H. Chen and W. Kinsner, "Texture segmentation using multifractal measures," in *Proc. WESCANEX*, May 22–23, 1997, pp. 222–227.
[23] A. Conci and L. H. Monteiro, "Multifractal characterization of texture-based segmentation," in *Proc. IEEE Int. Conf. Image Processing*, Vancouver, BC, Canada, Sep. 10–13, 2000, pp. 792–795.
[24] L. Kam and J. Blanc-Talon, "Are multifractal multipermuted multinomial measures good enough for unsupervised image segmentation," in *Proc. CVPR*, Hilton Head Island, NC, Jun. 13–15, 2000, pp. 58–63.
[25] I. Reljin, B. Reljin, I. Pavlovic, and I. Rakocevic, "Multifractal analysis of gray-scale images," in *Proc. Mediterranean Electrotechnical Conf.*, May 29–31, 2000, pp. 490–493.
[26] L. Houqiang, L. Zhengkai, and L. Feng, "Texture image segmentation method based on fractal theory and kohonen neural network," *Comput. Eng. Applicat. (Chinese)*, vol. 37, pp. 44–46, Jul. 2001.
[27] G. Du and T. S. Yeo, "A novel multifractal estimation method and its application to remote image segmentation," *IEEE Trans. Geosci. Remote Sens.*, vol. 40, no. 4, pp. 980–982, Jul. 2002.
[28] J. Feng, W.-C. Lin, and C.-T. Chen, "Fractal box-counting approach to fractal dimension estimation," in *Proc. IEEE Int. Conf. Pattern Recognition*, Vienna, Austria, Aug. 25–29, 1996, pp. 854–858.
[29] Q. Cheng, "The gliding box method for multifractal modeling," *Comput. Geosci.*, vol. 25, no. 9, pp. 1073–1079, 1999.
[30] P. Brodatz, *Texture: A Photographic Album for Artists and Designers*. New York: Dover, 1966.
[31] J. Serra, *Image Analysis and Mathematical Morphology (Vol. 1)*. New York: Academic, 1982.
[32] J. Samarabandu, R. Acharya, E. Hausmann, and K. Allen, "Analysis of bone x-rays using morphological fractals," *IEEE Trans. Med. Imag.*, vol. 12, no. 9, pp. 466–470, Sep. 1993.
[33] J. C. Bezdek, *Pattern Recognition With Fuzzy Objective Function Algorithms*. New York: Plenum Press, 1981.
[34] T. Kohonen, *Self-Organization Maps*. Berlin, Germany: Springer-Verlag, 1995.

Yong Xia (S'05) received the B.E. and M.E. degrees in computer application from Northwestern Polytechnical University, Xi'an, China, in 2001 and 2004, respectively. He is currently pursuing the Ph.D. degree at the School of Computers, Northwestern Polytechnical University, Xi'an, China.

From May 2003 to November 2003, he was a Research Assistant with the Center for Multimedia Signal Processing, Department of Electronic and Information Engineering, Hong Kong Polytechnic University, Hong Kong. Since 2004, he has been a Visiting Researcher with the School of Information Technologies, University of Sydney, Sydney, Australia. His research interests include image analysis, multimedia signal processing, pattern recognition, and machine learning.

(David) Dagan Feng (S'88–M'88–SM'94–F'03) received the Ph.D. degree in computer science from the University of California, Los Angeles (UCLA), in 1988.

After being an Assistant Professor in the U.S., he joined the University of Sydney, Sydney, Australia, as Lecturer, Senior Lecturer, Reader, and then Professor. He is the former Head of Department of Computer Science/School of Information Technologies. He is currently Associate Dean of the Faculty of Science and Director of the Biomedical and Multmedia Information (BMIT) Research Group, University of Sydney, and Professor and Deputy Director, Center for Multimedia Signal Processing, Department of Electronic and Information Engineering, Hong Kong Polytechnic University. He has published over 300 scholarly research papers, pioneered several new research directions, and made a number of landmark contributions in his field. More important, however, is that many of his research results have been translated into solutions to real-life problems worldwide and have made tremendous improvements to the quality of life.

Dr. Feng is a Fellow of ACS, HKIE, and IEE. He received the Crump Prize for Excellence in Medical Engineering. He is currently Special Area Editor of the IEEE TRANSACTIONS ON INFORMATION TECHNOLOGY IN BIOMEDICINE, Advisor for the *International Journal of Image and Graphics*, Chairman of IFAC-TC-BIOMED, and Chairman of the International Programme and National Organizing Committees for the IFAC 2003 Symposium.

Rongchun Zhao received the M.E. degree in weapon control and air force engineering from PLA's Institute of Military Engineering, Harbin, China, in 1960.

He was the Senior Visiting Scholar in the department of electric and electronic, Surrey University, Surrey, U.K., from 1989 to 1990. Currently, he is a Professor with the School of Computers, Northwestern Polytechnical University, Xi'an, China. He has been Head of the School of Computers and is currently a member of the Academic Committee of Northwestern Polytechnical University. His research interests include speech processing, image analysis and comprehension, computer vision, virtual reality, and pattern recognition. He has published more than 100 scholarly research papers and two monographs. He is the Founder and Director of the Provincial Key Laboratory of Speech and Image Information Processing (SIIP) at Northwestern Polytechnical University.

Mr. Zhao has been appointed as Vice President of China Society of Image and Graphics, Vice President of China Society of Stereology, Vice Director of the Signal Processing section of Chinese Institute of Electronics, and President of Shaanxi Signal Processing Association.